IOP Publishing Nanotechnology
Nanotechnology 33 (2022) 405404 (9pp) https://doi.org/10.1088/1361-6528/ac7883

Biological/metal oxide composite transport layers cast from green solvents for boosting light harvesting response of organic photovoltaic cells indoors

Janardan Dagar[1,2] **and Thomas M Brown**[1,*]

[1] CHOSE (Centre for Hybrid and Organic Solar Energy), Department of Electronic Engineering, University of Rome Tor Vergata, Via del Politecnico 1, I-00133 Rome, Italy
[2] Helmholtz-Zentrum Berlin, HySPRINT Innovation Lab, Kekuléstrasse 5, D-12489 Berlin, Germany

E-mail: thomas.brown@uniroma2.it

Received 4 March 2022, revised 20 May 2022
Accepted for publication 13 June 2022
Published 14 July 2022

Abstract

Organic solar cells with biological/metal–oxide electron transport layers (ETLs), consisting of a ZnO compact layer covered by a thin DNA layer, both of which deposited with green solvents (water or water/alcohols mixtures) are presented for application under low intensity indoor lighting. Under white LED lamp (200, 400 lx), photovoltaic cells with P3HT:$PC_{70}BM$ polymer semiconductor blends delivered an average maximum power density (MPD) of 8.7 μW cm^{-2}, corresponding to a power conversion efficiency, PCE, of = 8.56% (PCE of best cell was 8.74%). The ZnO/DNA bilayer boosted efficiency by 68% and 13% in relative terms compared to cells made with DNA-only and ZnO-only ETLs at 400 lx. Photovoltaic cells with ZnO/DNA composite ETLs based on PTB7:$PC_{70}BM$ blends, that absorb a broader range of the indoor lighting spectrum, delivered MPDs of 16.2 μW cm^{-2} with an estimated average PCE of 14.3% (best cell efficiency of 15.8%) at 400 lx. The best efficiencies for cells fabricated on flexible plastic substrates were 11.9% at 400 lx. This is the first report in which polymer photovoltaics incorporating biological materials have shown to increment performance at these low light levels and work very efficiently under indoor artificial light illumination. The finding can be useful for the production of more bio-compatible photovoltaics as well as bio-sensing devices based on organic semiconductors.

Keywords: DNA, polymer solar cell, organic solar cell, electron transport layer, green processing, indoor photovoltaics, biosensing

(Some figures may appear in colour only in the online journal)

Introduction

Polymer solar cells (PSCs) have received great interest due to their constant improvement in photovoltaic performance [1–5] and potential advantages including flexibility, being lightweight, low cost, and easy to fabricate [3, 6–8]. Several efforts have been made to improve the performance of PSCs in the last two decades [9–12]. Recently, PSCs and other new generation photovoltaics (PV) have been earmarked not only to be used for the conversion of natural sunlight but also of indoor artificial light [8, 13–15] to power applications such as the internet of things (autonomous sensors, health monitors, etc.) [16–18], and portable electronics [19, 20] as well as biosensing, artificial retina concepts, and biomedical devices [21–28]. The inverted device architecture consists of an electron extraction or transport layer (ETL) deposited on a bottom ITO electrode, a polymer blend, a hole extraction/transport layer (HTL), and a top metallic electrode. To achieve high performance, many efforts

* Author to whom any correspondence should be addressed.

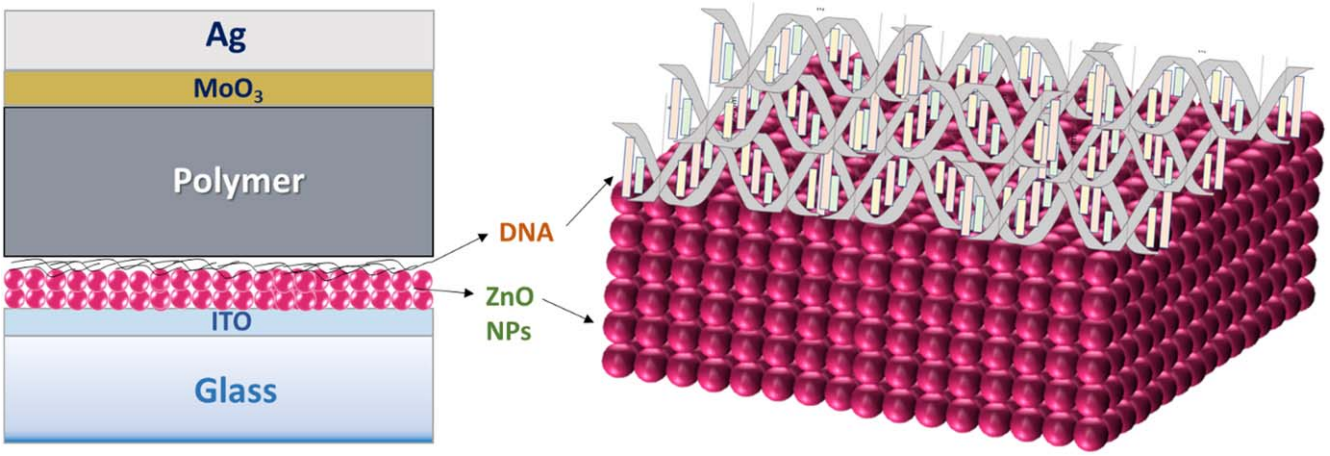

Figure 1. Inverted device architecture scheme of ITO/ETL/P3HT:$PC_{70}BM$ or PTB7:$PC_{70}BM$/MoO_3/Ag polymer solar cells fabricated in this study with different ETLs. The ETLs were DNA, ZnO, ZnO/DNA together with ITO only (without any ETL). The DNA-coated ZnO nanoparticle bilayer composite electron transport layer is highlighted in the schematic on the right.

have focused on developing high-quality electron extraction layers, including conjugated poly electrolytes [29, 30], metal oxides [31–36], fullerene derivatives [37–40], and even biological [41, 42] materials. Bio-derived layers [22, 41, 43–45], including DNA, have also been introduced in PSCs and in perovskite solar cells as an ETL [31, 46–48]. Hou *et al* [31] inserted DNA, additionally, in the active perovskite semiconductor with beneficial results even for hole transport and grain boundary passivation. ZnO is most commonly used ETL in PSCs because of its high electron mobility, low-temperature processing as well as high optical transparency [49, 50]. Nevertheless, because of the presence of surface defects and traps at its interfaces, solar cell performance has been shown to improve with the addition of a second layer together with ZnO. Such layers deposited with ZnO have included metal–oxide films [36], electrolytes [51, 52], 2D materials [53, 54], small organic molecules [55] as well as DNA [31] (studied only under standard test conditions). Here for the first time, we report the study of the influence of biological electron transport layers (ETLs) under indoor illumination. Since the optical power density is 2–3 orders of magnitude lower indoors compared to standard test conditions (i.e. 1 sun), the influence of the ETL under these low-light conditions is amplified and warrants a systematic study. These findings are particular relevant in applications of organic photovoltaics under low intensity light and indoor environments, which are required to be even more bio-compatible since direct handling by users will be more common, and extend more generally to biomedical devices such as heart rate detectors [56], powering devices under the skin [57], and even artificial retinas [21, 58] where interaction with biological materials as well as high efficiency for high performance over small areas are fundamental requirements.

Results and discussion

The device architecture of the PSCs was ITO/ZnO/DNA/polymer blend/MoO_3/Ag as shown in figure 1. The ETL consisted of a spin-coated ZnO nanoparticle film (ZnO-NPs) with average particle size $\leqslant$ 40 nm cast from a water and ethanol solution. We added a DNA film over ZnO-NPs ETL cast from a water and methanol solution. The polymer blend consisted of either a P3HT (Poly(3-hexylthiophen-2, 5-diyl)) or PTB7 (Poly[[4,8-bis[(2-ethylhexyl)oxy]benzo[1, 2-b:4, 5-b']dithiophene-2, 6-diyl][3-fluoro-2-[(2 ethylhexyl)carbonyl]thieno[3, 4-b]thiophenediyl]]) polymer donor mixed with $PC_{70}BM$ (6, 6]-Phenyl-C70-butyric acid methyl ester]) acceptor. MoO_3 and silver were thermally evaporated in succession as top electrode.

The current density–voltage characteristics of the best performing inverted P3HT:$PC_{70}BM$ solar cells with different ETLs, i.e. DNA, ZnO, ZnO/DNA together with ITO only (without any ETL), measured under *the intensity of* 400 lx *white light illumination*, which is the typical level found in office spaces, are shown in figure 2(a). The summary of average values of PV parameters such a short circuit current (J_{SC}), open circuit voltage (V_{OC}), Fill Factor (FF), PCE (power conversion efficiency) and maximum power density (MPD) are reported at both 200 lx (typical of home illumination) and 400 lx (typical office illumination) in tables 1(a) and (b). The values shown in table 1 are comparatively different from values measured under 1 sun illumination not only due to different 1.5 AM sun spectrum but also higher power density of the Sun [32]. The P3HT:$PC_{70}BM$ cells with ITO-only DNA, ZnO and ZnO/DNA composite layer delivered 1.17%, 3.22%, 3.43% and 4.09% average efficiencies respectively while measured under 1 sun illumination [32]. The PSC with DNA interlayer gave an average MPD of 5.20 μW cm^{-2} (corresponding to a PCE of 5.11%) at 400 lx white light illumination which is 43 times higher than the same cell with ITO only bottom electrode at 400 lx as a result of much lower recombination currents (figure 2(b)) and significantly higher difference between the work functions of the electron- and hole- collecting electrodes [59]. Single ETL ZnO based cells surpassed the performance of a single DNA ETL, yielding an average MPD value of 7.71 μW cm^{-2} (PCE = 7.59%). However, it is when both materials were combined in a ZnO/DNA composite ETLs that the best

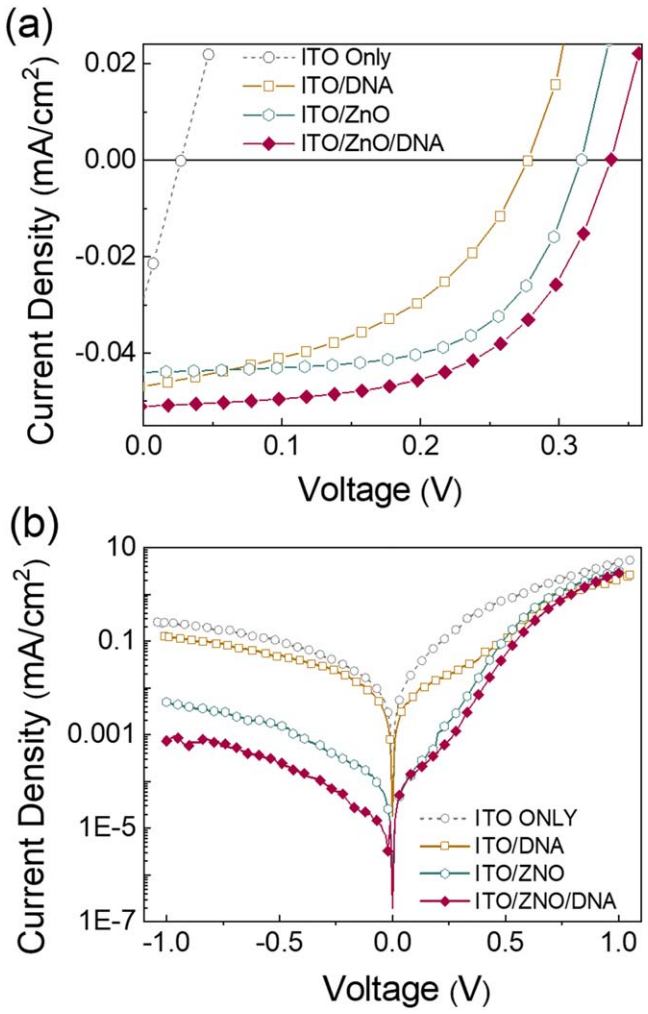

Figure 2. (a) current density–voltage (J–V) curves of the best P3HT:$PC_{70}BM$ polymer photovoltaic cells with different ETLs: ITO Only, DNA, ZnO and DNA-coated ZnO composite layer measured under the intensity of 400 lx white light illumination; (b) J–V curves of the same PV cells measured in the dark.

average MPD value of 8.70 μW cm^{-2} (corresponding to a PCE of 8.56%) was obtained at 400 lx. This is over double the efficiency at 1 sun. The performance at 200 lx follows the same trend closely, however the values are lower, a drop due to increase in leakage current [60, 61] reported from other literature studies on low level light measurements.

J–V characteristics in the dark of the best performing PSCs with different interlayers are plotted in figure 2(b). The on/off dark current ratio (at +1 V/−1 V) of 3.9 × 10^3 for PSCs with the ZnO/DNA composite ETL was at least a factor of 6 higher than that with only ZnO (on/off = 6.3 × 10^2) and only DNA (on/off = 1.8 × 10^1) as ETLs. Interestingly, the value of 10^3 has been suggested as a threshold for on/off ratios for obtaining high-performance devices under indoor illumination by Lucarelli *et al* [15]. Here, PSCs with ZnO only ETL come close but it is adding the DNA layer that surpass this value reflecting improved rectification behavior and lowest reverse current. The reverse current (at -1V), I_{off}, is more than an order of magnitude lower than devices with ITO- and DNA-only ETLs and 84% lower compared to the case with ZnO-only ETL, indicating that the DNA overlayer effectively reduces recombination currents which at low light intensities and photo-generated currents, is crucial [13, 15].

Series (R_S) and shunt resistance (R_{SH}) were calculated for cells with different ETLs and plotted in figure 3(a). The ZnO/DNA bilayer delivered the lowest average series resistance (R_S = 10.0 Ω cm^2) and maximum shunt resistance (R_{SH} = 0.88 kΩ cm^2) compared to ZnO ETL based solar cells confirming better hole blocking and electron-extracting behaviors for the ZnO/DNA bilayer ETL. To delve deeper on charge carrier recombination at the interface of ETL and polymer layer in organic solar cells, we carried out open circuit voltage decay (OCVD) measurements (figure 3(b)). Cells with ZnO/DNA bilayer take longer time to discharge (> 0.1 s) compared to the cells with ZnO and DNA only (0.01 s) indicating a reduction in density of defects which are responsible for unwanted charge recombination at the interface of ETL and polymer layer in PSCs.

Figure 3(c) shows the J–V characteristics of representative PTB7:$PC_{70}BM$ PSCs with ZnO/DNA ETL composite layer on both glass and flexible PET substrates. The mean value of the PV parameters including J_{SC}, V_{OC}, FF, PCE and MPD measured at 400 lx and 200 lx white LED light illumination are reported in table 2. Here we used PTB7:$PC_{70}BM$ polymer blend which absorbs a broader range of light compared to P3HT:$PC_{70}BM$ blend. Thus, PSCs with PTB7:$PC_{70}BM$ delivered improved PV parameters compared to those with P3HT:$PC_{70}BM$. The PTB7:$PC_{70}BM$ devices with ZnO/DNA composite layer on glass and flexible substrates delivered power conversion efficiencies of 8.31% and 7.06% respectively while measured under 1 sun illumination [31]. The ZnO/DNA interlayer based cells on glass substrate delivered average MPD = 16.2 μW cm^{-2} (corresponding to an average PCE of 14.3%) and on PET substrate delivered average MPD = 12.0 μW cm^{-2} (corresponding to an average PCE of 10.5%) measured at 400 lx white light LED illumination. Thus, there was a large boost in PCE of 72% for rigid and 49% for flexible in relative terms, at 400 lx indoor illumination levels compared to STC. The best cell efficiencies at 400 lx were 15.8% on glass and 11.9% on PET. Other PV parameters, together with the results at 200 lx, are reported in table 2. At 200 lx, the trend in performance between cells on glass and PET were similar to those at 400 lx, but with lower absolute values.

The energy level diagram of P3HT and PTB7:$PC_{70}BM$ PSCs with different ETLs, i.e. DNA, ZnO and DNA-coated ZnO composite bilayer together with ITO-only are shown in figures 4(a) and (b). In previous Kelvin probe measurements [31], it was shown that the work function (WF) of the ITO bottom electrode is reduced considerably after deposition of a DNA nano-layer, from 4.7 to 4.45 eV. The DNA layer also reduces, even if to a lesser extent, the work function of the ITO/ZnO from 4.30 to 4.25 eV which is the lowest value for the set of electrodes we developed. Lowering of the work function is a result of the DNA giving rise to an interfacial dipole. It is interesting to note that the V_{OC} of the solar cells (table 1) increases monotonically with the lowering of the electrode/ETL work function (figure 4). In fact, it has been shown that the built-in potential [36] as well as the V_{OC} of

Table 1. Summary of the PV parameters of P3HT:$PC_{70}BM$ polymer solar cells using different electron transport interlayers, i.e. DNA, ZnO, and ZnO/DNA composite, together with ITO-only measured under 200 lx and 400 lx white LED light illumination. In brackets we report the values for the best cell.

ETL	J_{sc} [μA cm^{-2}]	Voc [V]	FF [%]	P_{Max} [μW cm^{-2}]	PCE at 400 lx [%]	PCE at 1 Sun [%]
(a) Measured under 400 lx white LED light illumination. Also reported in the last column is the average efficiency at 1 sun						
ITO Only	27.9 ± 6.1 (28.8)	0.26 ± 0.004 (0.27)	18.3 ± 0.54 (19.0)	0.12 ± 0.08 (0.13)	0.11 ± 0.02 (0.13)	1.2
DNA	47.2 ± 1.50 (46.9)	0.275 ± 0.001 (0.277)	44.5 ± 0.45 (45.0)	5.20 ± 0.57 (5.27)	5.11 ± 0.05 (5.18)	3.2
ZnO	43.9 ± 0.73 (44.0)	0.316 ± 0.05 (0.316)	61.4 ± 0.4 (61.7)	7.71 ± 0.10 (7.73)	7.59 ± 0.01 (7.60)	3.4
ZnO/DNA	49.4 ± 0.02 (51.0.6)	0.339 ± 0.01 (0.337)	57.7 ± 1.92 (57.3)	8.70 ± 0.13 (8.89)	8.56 ± 0.13 (8.74)	4.1
ETL	J_{sc} [μA cm^{-2}]	Voc [V]	FF [%]	P_{Max} [μW cm^{-2}]	PCE at 200 lx [%]	
(b) Measured under the intensity of 200 lx white light irradiation						
ITO Only	20.4 ± 1.21 (20.5)	0.011 ± 0.001 (0.011)	0.77 ± 0.001 (0.69)	0.11 ± 0.002 (0.14)	0.017 ± 0.002 (0.015)	
DNA	20.1 ± 2.12 (20.7)	0.0140 ± 0.001 (0.014)	1.5 ± 0.001 (1.57)	0.25 ± 0.002 (0.27)	0.02 ± 0.001 (0.03)	
ZnO	20.3 ± 0.81 (20.7)	0.248 ± 0.01 (0.252)	33.1 ± 0.2 (35.07)	1.60 ± 0.01 (1.64)	2.30 ± 0.01 (2.36)	
ZnO/DNA	20.1 ± 0.01 (20.2)	0.290 ± 0.01 (0.292)	59.1 ± 1.01 (59.8)	3.01 ± 0.01 (3.20)	4.51 ± 0.11 (4.53)	

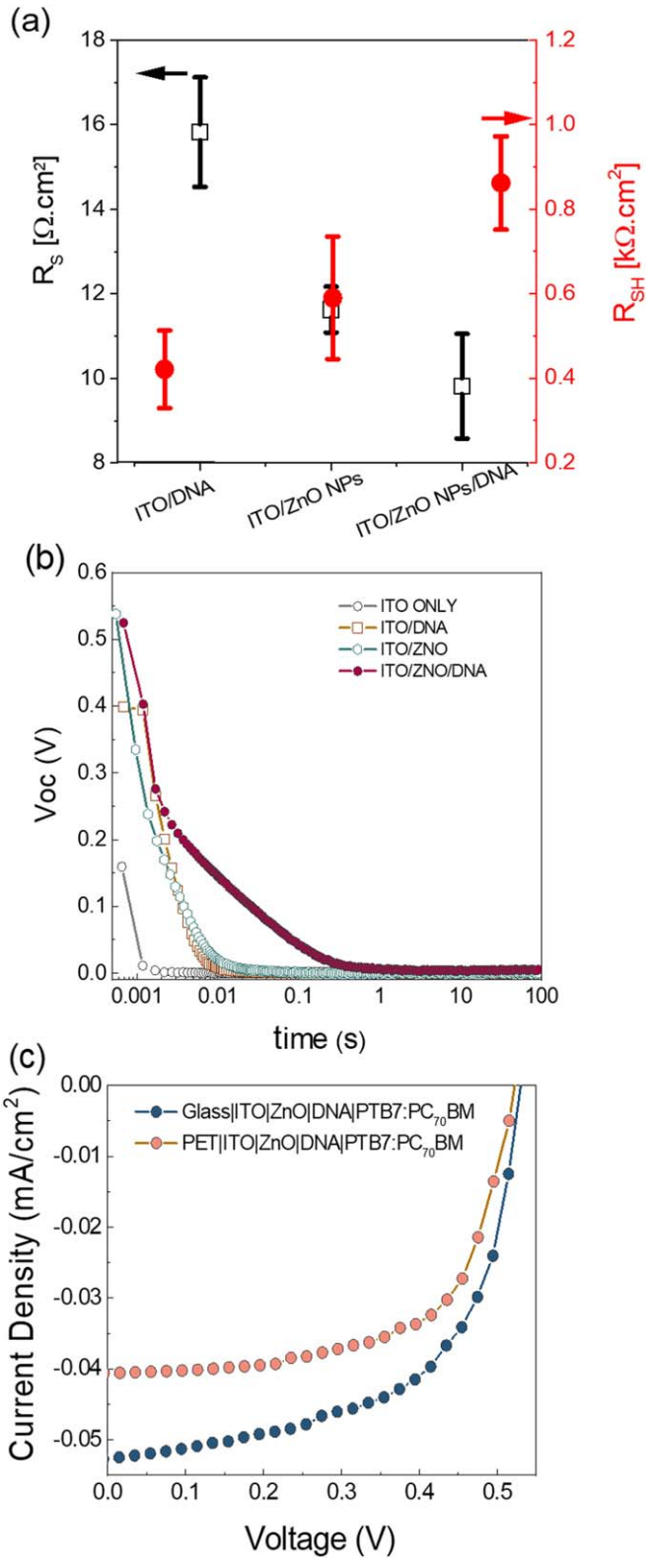

Figure 3. Shunt resistance (R_{SH}, closed circles) and series resistance (R_S, open squares) of P3HT:PC_{70}BM polymer solar cells using different electron transport interlayers: DNA, ZnO and ZnO/DNA, extracted from the *J–V* curves measured under 400 lx white LED light irradiation. (b) Open circuit voltage decay (OCVD) measurements. (c) *J–V* curves of best ITO/ZnO/DNA/PTB7:PC_{70}BM/MoO3/Ag solar cell devices fabricated on both glass and on PET substrates under the 400 lx white LED light illumination.

organic solar cells follows the work function variation of the electrodes [59]. Figure 4(c) shows the EQE spectra of P3HT:PC_{70}BM PSCs devices with different ETLs. We observed that EQE of ITO/ZnO/DNA ETL solar cells showed the highest EQE values compared to ITO/DNA and ITO/ZnO based solar cells, consistently with a higher driving force/built-in potential for charge separation and collection with these ETLs as well as DNA acting as a templating agent influencing blend morphology resulting in a larger delocalization of excitons and improved charge separation in such blends [32].

In conclusion, we fabricated P3HT:PC_{70}BM and PTB7:PC_{70}BM inverted PSCs with different ETLs including ZnO-NPs, DNA-only and DNA-coated DNA/ZnO composite layer and measured their performance under white LED indoor lighting at 200 lx and 400 lx. The P3HT:PC_{70}BM cells with ZnO/DNA bilayer delivered the highest MPD of 8.89 μW cm^{-2} corresponding to an efficiency of 8.74% at 400 lx. The ZnO/DNA bilayer boosted efficiency by 68% and 13% in relative terms compared to cells made with DNA-only and ZnO-only ETLs at 400 lx. Replacing P3HT with lower energy-gap PTB7 absorber donor layer increased light harvesting capabilities significantly further. The PTB7:PC_{70}BM inverted PSCs, which absorb the whole range of visible LED emission, with the ZnO/DNA composite ETL, delivered MPD of 16.2 μW cm^{-2} (corresponding estimated PCE = 14.3%) at 400 lx under indoor illumination with a best PCE of 15.8%. PSCs with same architecture but on PET substrates delivered MPDs of 12.0 μW cm^{-2} (corresponding estimated efficiency of 10.5%) at 400 lx under indoor illumination with the best flexible cells delivering a PCE = 11.9% at 400 lx. This is the first time PSCs that incorporate biological genetic material have been investigated for indoor applications. The findings can be useful not only for solar cells applications, where bio derived materials are introduced but can be useful for biosensing applications where conjugated polymer structures are also used.

Experimental

Materials

Zinc oxide nanoparticles (20 wt%. concentration in water and ethanol solution with average particle size $\leqslant$ 40 nm), DNA (Deoxyribonucleic acid) sodium salt extracted from salmon fish with molecular mass of 1.3 × 106 Da (~2000 base pair), Molybdenum oxide (MoO3, 99.98% powder), ortho-Xylene and silver (Ag, wire Z 99.99%) were purchased from Sigma Aldrich. P3HT (Poly(3-hexylthiophen-2, 5-diyl)), PTB7(Poly [[4, 8-bis[(2-ethylhexyl)oxy]benzo[1, 2-b:4, 5-b']dithiophene-2, 6-diyl][3-fluoro-2-[(2 ethylhexyl)carbonyl]thieno[3, 4-b]thiophenediyl]]) and PC70BM, [6, 6]-Phenyl-C71-butyric acid methyl ester, (99.99%) were purchased from Solarmer.

Table 2. Summary of the PV parameters of PTB7:$PC_{70}BM$ polymer solar cells using different electron transport interlayers like ZnO and ZnO/DNA composite via spin coning technique measured on glass substrates and flexible PET substrate under 400 lx and 200 lx white LED light irradiation. In brackets we report the values for the best cell. Also reported in the last column is the average efficiency at 1 sun.

ETL	Light source	J_{sc} [μA cm^{-2}]	Voc [V]	FF [%]	P_{Max} [μW cm^{-2}]	PCE indoors [%]	PCE at 1 sun [%]
Glass/ZnO/DNA	LED 200 lx	34.4 $\pm$ 1.77 (34.5)	0.458 $\pm$ 0.05 (0.461)	40.0 $\pm$ 2.18 (41.5)	6.12 $\pm$ 0.43 (6.62)	8.01 $\pm$ 0.55 (8.60)	8.3
Glass/ZnO/DNA	LED 400 lx	66.6 $\pm$ 0.51 (66.6)	0.491 $\pm$ 0.05 (0.496)	49.4 $\pm$ 3.50 (53.8)	16.2 $\pm$ 0.13 (17.9)	14.3 $\pm$ 1.18 (15.79)	8.3
PET/ZnO/DNA	LED 200 lx	20.4 $\pm$ 0.001 (20.4)	0.476 $\pm$ 0.01 (0.499)	49.24 $\pm$ 8.30 (61.0)	4.81 $\pm$ 0.1 (6.21)	6.25 $\pm$ 1.25 (8.07)	7.1
PET/ZnO/DNA	LED 400 lx	39.6 $\pm$ 0.01 (40.6)	0.510 $\pm$ 0.01 (0.515)	59.0 $\pm$ 5.28 (54.2)	12.0 $\pm$ 0.13 (13.5)	10.5 $\pm$ 1.20 (11.9)	7.1

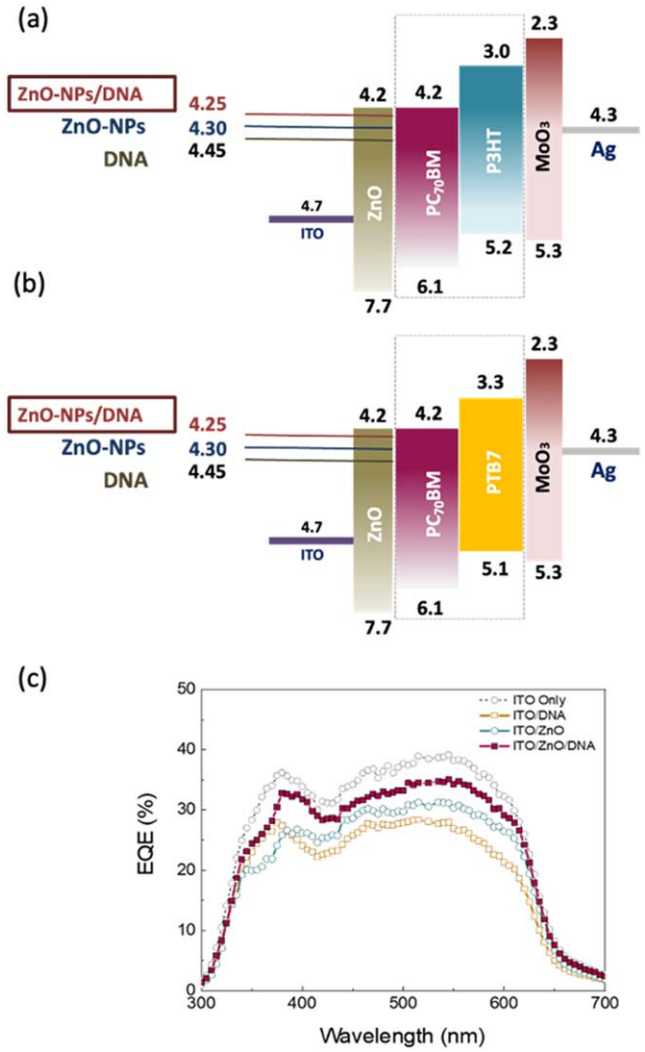

Figure 4. Energy level diagrams of (a) P3HT:$PC_{70}BM$ and (b) PTB7:$PC_{70}BM$ polymer photovoltaic cells with different ETLs: ITO-Only, DNA, ZnO and DNA-coated ZnO bilayer; (c) EQE diagram of different ETL based P3HT:$PC_{70}BM$ polymer solar cells.

Solar cell device fabrication

For the fabrication of inverted solar cell devices, glass/ITO and PET/ITO substrates were patterned with wet-etching in hydrobromic acid (HBr). The etched glass/ITO substrates were cleaned with ultrasonication in acetone and 2-proponol for 10 min in each solvent. The patterned PET/ITO substrates were cleaned with ethanol for 10 min in ultrasonication. PSCs with the structure of ITO/ZnO-NPs/DNA/P3HT or PTB7:$PC_{70}BM$/MoO_3/Ag were fabricated. Firstly, the ZnO- nanoparticles solution was prepared via diluting the ZnO dispersion with 10 μl ml^{-1} concentration in ethanol in air and kept on stirring overnight at room temperature. The ZnO-NPs thin film was prepared via spinning the solution with the spin speed of 2500 rpm on cleaned rigid (glass/ITO) and flexible (PET/ITO) substrates and then annealed at 140 °C for 20 min in air. The thickness of ZnO NPs thin film over ITO electrode was 50 nm calculated by profilometer (Dektak 150). In the next sept, DNA solution was prepared according to recipe reported previously [31]. The DNA solution was deposited on glass/ITO or PET/ITO substrates or ZnO-NPs layer (Glass or PET/ZnO/DNA) and dried overnight in vacuum. The polymer blend layer P3HT:$PC_{70}BM$ (1:0.7) was dissolved in 20 mg ml^{-1} in ortho-dichlorobenzene and stirred at 75 °C temperature overnight in N_2 atmosphere. The polymer blend solution was spin coated at 500 rpm and annealed at a temperature of 130 °C for 10 min. PTB7:$PC_{70}BM$ (1:1.5) polymer blend was dissolved in ortho-xylene and 3% v/v of 1, 8-diiodooctane (DIO) and the solution was deposited on 500 rpm for 80 s and with 1500 rpm for next 10 s and then wet films were dried in vacuum.

Subsequently, the active layer coated substrates were loaded in the metal thermal evaporator where 5 nm thick MoO_3 hole extracting interlayer was thermally deposited. Silver (Ag) as top electrode with 100 nm thickness was evaporated thermally using a shadow mask.

Device measurements:

To perform the *J-V* measurements of PSCs under indoor light illumination, a home made setup consists of a fixed light source (white light LED lamp) was utilized. Different light irradiance levels of 200 lx and 400 lx were determined via varying the distance of the samples from the light source, as reported in [62]. To establish the different light irradiance conditions, Digisense 20250-00 light meter was used which is provided with NIST (National Institute of Standard and Technology) traceable calibration. In addition, the irradiance spectrum was measured with the International Light Technologies ILT900 spectroradiometer which also has a NIST-traceable calibration in order to determine the optical power at each of the different lux employed during measurements. PSCs were masked with a black tape with 0.1 cm^2 area. IPCE-LS200, Dyers system was used to measure EQE spectra.

Arkeo was used to measure the irradiance intensity dependence of Voc and Jsc, the Voc decay times, and the dark *J–V* characteristics of the solar cells as shown in a previous study [14].

Acknowledgments

We thank Manuela Scarselli, Maurizio De Crescenzi, Guido Scavia, Silvia Destri, Francesco Toschi, Daniele Catone, Patrick O'Keeffe, Alessandra Paladini, Stefano Turchini, Dario Di Carlo Rasi, Andrea Zampetti, Sergio Alexis Castro Hermosa, Matteo Gasbarri, Luca La Notte, Giampaolo Susanna, Francesca Brunetti, Andrea Reale and Aldo Di Carlo and Shashank Priya for useful discussions. This work was supported by the Air Force Office of Scientific Research's Biophysics program through award number FA9550-20-1-0157.

Data availability statement

All data that support the findings of this study are included within the article (and any supplementary files).

ORCID iDs

Thomas M Brown https://orcid.org/0000-0003-2141-3587

References

[1] h. w. n. g. p. c.-e. h. a. Best Research-Cell Efficiency Chart (https://nrel.gov/pv/cell-efficiency.html)

[2] Mainville M and Leclerc M 2020 Recent progress on indoor organic photovoltaics: from molecular design to production scale *ACS Energy Lett.* **5** 1186–97

[3] Dincer I 2000 Renewable energy and sustainable development: a crucial review *Renewable Sustain. Energy Rev.* **4** 157–75 2000/06/01/

[4] Lai W-C, Lin K-W, Guo T-F, Chen P and Liao Y-Y 2018 Efficient $CH_3NH_3PbI_3$ perovskite/fullerene planar heterojunction hybrid solar cells with oxidized Ni/Au/Cu transparent electrode *Appl. Phys. Lett.* **112** 071103

[5] Li B, Hou B and Amaratunga G A J 2021 Indoor photovoltaics, the next big trend in solution-processed solar cells *InfoMat* **3** 445–59

[6] Dai S and Zhan X 2018 Nonfullerene acceptors for semitransparent organic solar cells *Adv. Energy Mater.* **8** 1800002

[7] Kaltenbrunner M *et al* 2012 Ultrathin and lightweight organic solar cells with high flexibility *Nat. Commun.* **3** 770

[8] Dagar J *et al* 2018 Efficient fully laser-patterned flexible perovskite modules and solar cells based on low-temperature solution-processed SnO_2/mesoporous-TiO_2 electron transport layers *Nano Res.* **11** 2669–81

[9] Liu Q *et al* 2020 18% Efficiency organic solar cells *Sci. Bull.* **65** 272–5

[10] Ikram M, Murray R, Hussain A, Ali S and Ismat Shah S 2014 Hybrid organic solar cells using both ZnO and PCBM as electron acceptor materials *Mater. Sci. Eng.* B **189** 64–9

[11] Imran M, Ikram M, Anjum S, Ali S and Huang Y 2018 Highly efficient hybrid bulk heterojunction organic solar cells integrating PbS nanoparticles *Nanosci. Nanotechnol. Lett.* **10** 1644–50 //

[12] Ikram M, Murray R, Imran M, Ali S and Shah S I 2016 Enhanced performance of P_3HT/(PCBM:ZnO:TiO_2) blend based hybrid organic solar cells *Mater. Res. Bull.* **75** 35–40

[13] Di Giacomo F *et al* 2016 Mesoporous perovskite solar cells and the role of nanoscale compact layers for remarkable all-round high efficiency under both indoor and outdoor illumination *Nano Energy* **30** 460–9

[14] Dagar J, Castro-Hermosa S, Lucarelli G, Cacialli F and Brown T M 2018 Highly efficient perovskite solar cells for light harvesting under indoor illumination via solution processed SnO2/MgO composite electron transport layers *Nano Energy* **49** 290–9

[15] Lucarelli G, Di Giacomo F, Zardetto V, Creatore M and Brown T M 2017 Efficient light harvesting from flexible perovskite solar cells under indoor white light-emitting diode illumination *Nano Res.* **10** 2130–45

[16] Pecunia V, Occhipinti L G and Hoye R L Z 2021 Emerging indoor photovoltaic technologies for sustainable internet of things *Adv. Energy Mater.* **11** 2100698

[17] Peng Y *et al* 2021 Lead-free perovskite-inspired absorbers for indoor photovoltaics *Adv. Energy Mater.* **11** 2002761

[18] Mathews I, Kantareddy S N, Buonassisi T and Peters I M 2019 Technology and market perspective for indoor photovoltaic cells *Joule* **3** 1415–26

[19] Yang S-S, Hsieh Z-C, Keshtov M L, Sharma G D and Chen F-C 2017 Toward high-performance polymer photovoltaic devices for low-power indoor applications *Solar RRL* **1** 1700174

[20] Wu J-L, Chen F-C, Chuang M-K and Tan K-S 2011 Near-infrared laser-driven polymer photovoltaic devices and their biomedical applications *Energy Environ. Sci.* **4** 3374–8

[21] Ciocca M *et al* 2020 Colour-sensitive conjugated polymer inkjet-printed pixelated artificial retina model studied via a bio-hybrid photovoltaic device *Sci. Rep.* **10** 21457

[22] Pradhan S, Brooks A K and Yadavalli V K 2020 Nature-derived materials for the fabrication of functional biodevices *Mater. Today Bio.* **7** 100065

[23] Liao C, Zhang M, Yao M Y, Hua T, Li L and Yan F 2015 Flexible organic electronics in biology: materials and devices *Adv. Mater.* **27** 7493–527

[24] Lanzani G 2014 Organic electronics meets biology *Nat. Mater.* **13** 775–6

[25] Owens R M and Malliaras G G 2011 Organic electronics at the interface with biology *MRS Bull.* **35** 449–56

[26] Ghezzi D, Antognazza M R, Dal Maschio M, Lanzarini E, Benfenati F and Lanzani G 2011 A hybrid bioorganic interface for neuronal photoactivation *Nat. Commun.* **2** 166

[27] Maya-Vetencourt J F *et al* 2020 Subretinally injected semiconducting polymer nanoparticles rescue vision in a rat model of retinal dystrophy *Nat. Nanotechnol.* **15** 698–708

[28] Chenais N A L, Airaghi Leccardi M J I and Ghezzi D 2021 Photovoltaic retinal prosthesis restores high-resolution responses to single-pixel stimulation in blind retinas *Commun. Mater.* **2** 28

[29] Yip H L and Jen A K Y 2012 Recent advances in solution-processed interfacial materials for efficient and stable polymer solar cells *Energy Environ. Sci.* **5** 5994–6011

[30] Susanna G *et al* 2015 8.7% Power conversion efficiency polymer solar cell realized with non-chlorinated solvents *Solar Energy Mater. Solar Cells* **134** 194–8

[31] Dagar J, Scavia G, Scarselli M, Destri S, De Crescenzi M and Brown T M 2017 Coating ZnO nanoparticle films with DNA nanolayers for enhancing the electron extracting properties and performance of polymer solar cells *Nanoscale* **9** 19031–8

[32] Toschi F *et al* 2018 Enhanced charge separation efficiency in DNA templated polymer solar cells *Adv. Funct. Mater.* **28** 1707126

[33] Xie J *et al* 2019 Solution-processed ZnO/MoS_2 quantum dots electron extraction layer for high performance inverted organic photovoltaics *Org. Electron.* **75** 105381

[34] Bhardwaj R, Bharti A, Singh J P, Chae K H and Goyal N 2020 Influence of Cu doping on the local electronic and magnetic properties of ZnO nanostructures *Nanoscale Adv.* **2** 4450–63

[35] Peng X *et al* 2020 Enhanced performance of perovskite solar cells using DNA-doped mesoporous-TiO2 as electron transporting layer *Sol. Energy* **206** 855–63

[36] Ierides I, Squires I, Lucarelli G, Brown T M and Cacialli F 2021 Inverted organic photovoltaics with a solution-processed ZnO/MgO electron transport bilayer *J. Mater. Chem.* C **9** 3901–10

[37] Punzi A *et al* 2016 'Synthetic routes to teg-substituted diketopyrrolopyrrole-based low band-gap polymers *Eur. J. Org. Chem.* pp 3233–42 **2016**

[38] Dagar J *et al* 2021 'Compositional and interfacial engineering yield high-performance and stable p-i-n perovskite solar cells and mini-modules *ACS Appl. Mater. Interfaces* **13** 13022–33

[39] Cho S *et al* 2014 Role of additional PCBM layer between ZnO and photoactive layers in inverted bulk-heterojunction solar cells *Sci. Rep.* **4** 4306

[40] Ikram M, Ali S, Murray R, Hussain A, Islah U D and Shah S I 2015 Influence of fullerene derivative replacement with TiO_2 nanoparticles in organic bulk heterojunction solar cells *Curr. Appl Phys.* **15** 48–54

[41] Cavinato L M, Fresta E, Ferrara S and Costa R D 2021 Merging biology and photovoltaics: how nature helps sun-catching *Adv. Energy Mater.* **11** 2100520
[42] Liu M *et al* 2021 Natural biomaterial sarcosine as an interfacial layer enables inverted organic solar cells to exhibit over 16.4% efficiency *Nanoscale* **13** 11128–37
[43] Yoon J *et al* 2021 'Bio-inspired strategies for next-generation perovskite solar mobile power sources,' *Chem. Soc. Rev.* **50** 12915–84
[44] Liang L, Fu Y, Wang D, Wei Y, Kobayashi N and Minari T 2018 DNA as functional material in organic-based electronics *Appl. Sci.* **8** 90
[45] Gao Z, Zhang X, Yu J and Yu X 2019 Bio-inspired materials as interfacial layers for high performance perovskite photodetectors *Opt. Mater. Express* **9** 3968–76
[46] Dagar J, Scarselli M, De Crescenzi M and Brown T M 2016 Solar cells incorporating water/alcohol-soluble electron-extracting DNA nanolayers *ACS Energy Lett.* **1** 510–5
[47] Hou Y *et al* 2019 Enhanced performance and stability in DNA-perovskite heterostructure-based solar cells *ACS Energy Lett.* **4** 2646–55
[48] Elfwing A *et al* 2018 DNA based hybrid material for interface engineering in polymer solar cells *ACS Appl. Mater. Interfaces* **10** 9579–86
[49] Chen L-M, Hong Z, Li G and Yang Y 2009 Recent progress in polymer solar cells: manipulation of polymer:fullerene morphology and the formation of efficient inverted polymer solar cells *Adv. Mater.* **21** 1434–49
[50] Gao Z *et al* 2019 Passivating ZnO with a naphthalimide-Schiff base as electron transport layer for inverted polymer solar cells *Org. Electron.* **67** 232–6
[51] Kim Y H, Kim D G, Maduwu R D, Jin H C, Moon D K and Kim J H 2018 Organic electrolytes doped ZnO Layer as the electron transport layer for bulk heterojunction polymer solar cells *Sol. RRL* **2** 1800086
[52] Guillén E *et al* 2011 ZnO-based dye solar cell with pure ionic-liquid electrolyte and organic sensitizer: the relevance of the dye–oxide interaction in an ionic-liquid medium *Phys. Chem. Chem. Phys.* **13** 207–13
[53] Liang Z *et al* 2013 Growth of vertically aligned ZnO nanowalls for inverted polymer solar cells *Sol. Energy Mater. Sol. Cells* **117** 34–40
[54] Huang Y J, Chen H C, Lin H K and Wei K H 2018 Doping ZnO electron transport layers with MoS_2 nanosheets enhances the efficiency of polymer solar cells *ACS Appl. Mater. Interfaces* **10** 20196–204
[55] Ruankham P, Macaraig L, Sagawa T, Nakazumi H and Yoshikawa S 2011 Surface modification of ZnO nanorods with small organic molecular dyes for polymer–inorganic hybrid solar cells *J. Phys. Chem.* C **115** 23809–16
[56] Cui N *et al* 2021 Stretchable transparent electrodes for conformable wearable organic photovoltaic devices *npj Flexible Electron.* **5** 31
[57] Chen F-C 2019 Emerging organic and organic/inorganic hybrid photovoltaic devices for specialty applications: low-level-lighting energy conversion and biomedical treatment *Adv. Opt. Mater.* **7** 1800662
[58] Ghezzi D *et al* 2013 A polymer optoelectronic interface restores light sensitivity in blind rat retinas *Nat. Photon.* **7** 400–6
[59] Zampetti A *et al* 2015 Influence of the interface material layers and semiconductor energetic disorder on the open circuit voltage in polymer solar cells *J. Polym. Sci.* B **53** 690–9
[60] Lechêne B P, Cowell M, Pierre A, Evans J W, Wright P K and Arias A C 2016 Organic solar cells and fully printed super-capacitors optimized for indoor light energy harvesting *Nano Energy* **26** 631–40
[61] Proctor C M and Nguyen T-Q 2015 Effect of leakage current and shunt resistance on the light intensity dependence of organic solar cells *Appl. Phys. Lett.* **106** 083301
[62] De Rossi F, Pontecorvo T and Brown T M 2015 Characterization of photovoltaic devices for indoor light harvesting and customization of flexible dye solar cells to deliver superior efficiency under artificial lighting *Appl. Energy* **156** 413–22